

# Chronic Unpredictable Stress Reduces Immunostaining for Connexins 43 and 30 and Myelin Basic Protein in the Rat Prelimbic and Orbitofrontal Cortices

José Javier Miguel-Hidalgo , Mohadetheh Moulana, Preston Hardin Deloach, and Grazyna Rajkowska

## Abstract

**Background:** Astrocytes and oligodendrocytes are pathologically altered in dorsolateral prefrontal and orbitofrontal cortices in major depressive disorder. In rat models of stress (major depressive disorder risk factor) astrocyte gap junction protein connexin 43 (Cx43) is reduced in the prelimbic cortex. Astrocyte connexins are recognized to strongly influence myelin maintenance in the central nervous system. However, it is unknown whether stress-related changes in Cx43 and the other major astrocyte connexin, Cx30, occur in the orbitofrontal cortex, or whether connexin changes are concurrent with disturbances in myelination.

**Methods:** Frozen sections containing prelimbic cortex and orbitofrontal cortex of rats subjected to 35 days of chronic unpredictable stress and controls ( $n = 6/\text{group}$ ) were immunolabeled for Cx43, Cx30, and myelin basic protein. Density of Cx43 or Cx30 immunoreactive puncta and area fraction of myelin basic protein immunoreactivity were measured in prelimbic cortex and orbitofrontal cortex and results analyzed with  $t$  test or Pearson correlations.

**Results:** Density of Cx43- and Cx30-positive puncta in both prelimbic cortex and orbitofrontal cortex was lower in chronic unpredictable stress-treated than in control rats. In both regions, the area fraction of myelin basic protein immunoreactivity was also lower in chronic unpredictable stress animals. Myelin basic protein area fraction was positively correlated with the density of Cx43-positive puncta in orbitofrontal cortex, and with Cx30 puncta in prelimbic cortex.

**Conclusion:** Low Cx43 and Cx30 after chronic unpredictable stress in rat prelimbic cortex and orbitofrontal cortex suggests that reduced astrocytic gap junction density may generalize to the entire prefrontal cortex. Concurrent reduction of Cx43-, Cx30-, and myelin basic protein-immunolabeled structures is consistent with a mechanism linking changes in astrocyte gap junction proteins and disturbed myelin morphology in depression.

## Keywords

prefrontal cortex, major depressive disorder, oligodendrocytes, astrocytes, stress, myelin, connexin

Received 7 September 2018; Accepted 22 October 2018

## Introduction

Exposure to repeated or prolonged periods of stress strongly increases the risk for developing major depressive disorder (MDD) in humans.<sup>1–4</sup> In rodent models as well, mild, chronic unpredictable stress (CUS) over a few weeks results in behaviors with both reasonable face validity for depression symptoms and predictive validity for the effects of antidepressants.<sup>5–9</sup> In human postmortem studies, accumulating evidence indicates that, beyond neuronal pathology, morphological and molecular glial

cell markers are significantly altered in areas of the prefrontal cortex (PFC) and other depression-relevant brain regions,<sup>10–13</sup> suggesting that functional disturbances in

<sup>1</sup>University of Mississippi Medical Center, Jackson, MS, USA

### Corresponding author:

José Javier Miguel-Hidalgo, Department of Psychiatry and Human Behavior, University of Mississippi Medical Center, 2500 N. State Street, Jackson, MS 39216, USA.

Email: [jmiguel-hidalgo@umc.edu](mailto:jmiguel-hidalgo@umc.edu)



depression may be partly mediated by glial anomalies. In regions of the rodent brain homologous to the human PFC, prolonged stress exposure also results in anomalous molecular and structural changes of astrocytes and other glial cells, while damage to these cells recapitulates depression-like behavioral alterations.<sup>14</sup>

In the brain of MDD subjects, lower levels of connexins 43 and 30, the major gap junction proteins expressed in astrocytes, or their messenger RNAs (mRNAs) have been detected in the dorsolateral PFC,<sup>15</sup> while similar reductions of Cx43 levels and density of Cx43 immunoreactive aggregates have been also described in the orbitofrontal cortex (OFC).<sup>16</sup> Furthermore, reduced mRNA levels of some myelin-related proteins have also been found in the OFC of subjects with MDD.<sup>17,18</sup> In rodents, CUS causes significant depression-like behaviors and reduction of Cx43 and gap junction communication in the prelimbic cortex (PLC), which are all prevented by treatment with corticosteroid receptor blockers.<sup>19</sup> Stress-related situations such as social isolation have been shown to reversibly reduce structural indices of myelination in the PLC, a medial region of the rat PFC, but not in other brain regions.<sup>20</sup> Other recent reports have also shown that CUS causes morphological alterations in the morphology of oligodendrocytes and the nodes of Ranvier in the corpus callosum.<sup>21</sup> It is unknown, however, whether gap junction or myelin changes occur in the rodent OFC after CUS or other procedures that cause depression-like behaviors.

Part of the relevance of putative concurrent changes in myelin markers and in astrocyte gap junction proteins Cx43 and Cx30 in stress-related disorders stems from the importance of these two connexins to the formation and maintenance of myelin. Myelin is a major factor for fast, reliable propagation of action potentials,<sup>22</sup> suggesting a possible connectivity-based mechanism by which stress or other factors may contribute to depression.<sup>23,24</sup> Cx43 and Cx30 subunits spanning the astrocyte cell membrane form heterotypical gap junctions with connexins 47 and 32 in oligodendrocyte cell membranes, allowing for direct communication between the cytoplasm of adjacent oligodendrocytes and astrocytes.<sup>22,25</sup> In fact, conditional knockout of Cx43 and Cx30 leads to severe alterations of myelin structure and motor functions in rodents.<sup>26</sup> Demyelination is not a hallmark of depression, but alterations in Cx43 or Cx30 may result in milder but significant changes in the thickness of myelin or the levels and distribution of myelin proteins and thus affect the propagation of action potentials, which may contribute to alterations of functional connectivity between PFC and other brain regions.<sup>27,28</sup> The research reported in this article sought to determine whether myelinated fibers immunohistochemically identified with specific antibodies to myelin basic protein (MBP), and aggregates of Cx43 or Cx30 immunoreactivity, were significantly

decreased in CUS-exposed rats as compared to nonexposed rats. In addition, we were interested in determining whether alterations in the distribution of those proteins are limited to the PLC or also occur in the rat OFC, as pathology in these two well-differentiated rat prefrontal cortical regions has been implicated in different aspects of depression-like behaviors.<sup>14,29–33</sup>

## Methods

### Animals

For this study, 12 adult male Sprague–Dawley rats weighing 200 to 250 g, obtained from Charles River, Wilmington, MA, were first acclimated for one week to the laboratory animal facilities. Rats were then split into CUS and control groups ( $n = 6$  per group). Animals in the CUS group were treated for 35 days with CUS according to the protocol detailed in previous publications,<sup>33,34</sup> and in the control group they were only shortly handled and returned to their cages daily during the same 35-day period. Sucrose preference and novelty-suppressed feeding were tested and recorded in CUS-treated and control rats by researchers naïve to the treatment group as previously described.<sup>34</sup> Protocols and procedures were performed in accordance with the guidelines and regulations of the Institutional Animal Care and Use Committee and the National Institutes of Health. Body weight was measured on day 0, two days after the beginning of CUS, and every four days thereafter. Sucrose preference was tested starting three weeks into the CUS treatment and novelty suppressed feeding at the end of the CUS period.

The rats in this study were the same as the ones used in our previous study on the glial fibrillary acidic protein immunoreactive astrocytes in the white matter of rat PLC in which we randomly selected six rats per group for immunohistochemical determinations (out of a total of 10 rats subjected to CUS and 10 control rats).<sup>33</sup> Histological sections in this study were adjacent to the sections for glial fibrillary acidic protein-related white matter determinations in the published research<sup>33</sup> but treated according with the immunohistochemical protocols detailed in the following section.

### Immunohistochemistry

After the CUS procedure, animals were euthanized and their brains immediately removed, flash-frozen in dry ice-cold isopentane and stored at  $-80^{\circ}\text{C}$  until sectioning. Fresh-frozen, coronal histological sections at a thickness of  $20\text{ }\mu\text{m}$  were made in a cryostat at  $-20^{\circ}\text{C}$ , mounted on coated slides and stored at  $-80^{\circ}\text{C}$  until immunohistochemical processing. For immunohistochemistry, sections were removed from the freezer and immediately allowed

to dry at room temperature for 20 min, fixed with 4% paraformaldehyde for 15 min, and washed once in 0.1 M phosphate buffer saline, pH 7.4 and twice in 0.1 M Tris-HCl buffer saline solution (TBS), pH 7.6 for 10 min each time. Slides were laid flat, and sections were encircled by PAP-PEN and treated with a preincubation solution containing 0.2% Triton-X and 2% bovine serum albumin in TBS. Antibodies for MBP (polyclonal antibody made in chicken, catalog #AB9348, working dilution 1:200; Millipore, Temecula, CA), connexin 43 (monoclonal antibody made in mouse, catalog # 610062, BD Bioscience, working dilution 1:300; Franklin Lakes, NJ) or connexin 30 (polyclonal antibody Z-PP9 made in rabbit, catalog # 71-2200, Thermo Fisher Scientific, working dilution 1:300) were then diluted in preincubation solution and this antibody solution applied to the section for overnight incubation in a refrigerator. Then the sections were washed three times in TBS and incubated in a solution with a biotinylated secondary antibody directed to the species of the first antibody at a 1:200 dilution. After three further washes in TBS, sections were incubated in preincubation solution containing a peroxidase-based ABC complex prepared in TBS according to the supplier instructions (Vector Laboratories, Burlingame, CA). After three more TBS washes, biotinylated antibody complexes were revealed incubating the sections for 5 min with a TBS solution containing 0.05% diaminobenzidine, 0.6% ammonium nickel sulfate, and 0.0045%  $\text{H}_2\text{O}_2$  at room temperature. Sections were then washed in TBS three times, dehydrated in an increasing series of water-diluted ethanol, then in absolute ethanol and xylene, and coverslipped with a permanent mounting medium. In each experiment, equal numbers of sections from each experimental group were simultaneously processed using the same antibody and buffer solutions.

## Morphometric Analyses

### *Packing Density of Cx43 and Cx30 Immunoreactive Puncta*

The density of immunoreactive puncta for Cx43 and Cx30 was measured in the PLC and OFC in the three sampled sections (see above) using a series of three-dimensional counting frames within the region of interest (picture frame as above) under a  $100\times$  oil objective (1.4 numerical aperture). Sampling of counting frames within the region of interest in the PLC or OFC resulted in the selection of between 12 and 20 counting three-dimensional frames (50- $\mu\text{m}$  wide, 50- $\mu\text{m}$  high, and 4- $\mu\text{m}$  thick) per brain area per section. All immunoreactive puncta within each counting frame were counted according to the optical disector rules using the StereoInvestigator software (MBF Biosciences, version

2017.01.0, Williston, VT) and eventually calculated as the number of puncta within the volume of tissue of all the frames within each region of interest of a section and expressed as a packing density (puncta/ $\text{mm}^3$ ). The density of immunoreactive puncta was averaged among the three sections of a subject to obtain a value of density of immunoreactive puncta per subject. This averaged density per subject was then considered a value for the packing density variable used in further statistical analysis. Measurements of packing density of connexin-immunoreactive puncta and area fraction of MBP immunoreactivity were made blind to the experimental group of the slide containing the measured histological sections.

### *Area Fraction of MBP Immunoreactive Fibers*

MBP-immunostained sections were visualized under a brightfield microscope. Three sections separated by 200- $\mu\text{m}$  intervals were selected randomly starting among the first 60  $\mu\text{m}$  of the rat frontal pole, and pictures were taken centered on the PLC that included all cortical layers from the medial brain surface until short of the border with the white matter. All picture frames had the same dimensions (800  $\times$  800  $\mu\text{m}$ ). As can be appreciated in Figure 3, the nonimmunoreactive background within the gray matter was devoid of any significant immunostaining. Intensity of the microscope illumination was maintained constant for all sections. Immunoreactive structures were then digitized using a cut off of 20 illumination intensity values over the nonspecific background as measured with the image analysis software ImageJ (out of 256 possible illumination values allowed, 0 represents maximum illumination light transmitted and 255 the lowest level of illumination, with a higher number indicating higher level of MBP immunoreactivity). The 20 levels of illumination cut-off applied to all sections were used as a threshold to obtain a binary image of MBP-immunoreactive structures (darker) against the nonimmunoreactive background (lighter). Then the area occupied by the immunoreactive structures within the bidimensional frame of the picture was measured and expressed as a percentage of the total area of the picture frame (that percentage called herein area fraction). The area fractions of the three frames per brain region (PLC or OFC) were used to obtain an average area fraction for each subject. These averages were then considered the values for the area fraction of MBP immunoreactivity variable used in statistical comparisons.

### *Statistics*

Values of packing densities of Cx43 and Cx30 immunoreactive puncta and of MBP area fraction of immunoreactivity (expressed as a percentage) were used as variables in the statistical analysis. The behavioral variables examined

were mean latency to feed in a novel environment and sucrose preference measured as the ratio of the consumption of an aqueous 3% sucrose solution to plain water. The variables were compared between CUS exposed and nonexposed groups using a two-tailed Student's *t* test. Differences between groups were considered significant at  $p < 0.05$ . Possible correlation between packing density of connexins and area fraction of MBP was studied with Pearson correlation analysis and considered significant at  $p < 0.05$ . Pearson correlation analysis was also used to study possible correlation between morphometric measurements of immunoreactivity and results of behavioral tests.

## Results

### *Packing Density of Cx43 and Cx30 Puncta*

We compared two different antibodies for Cx43 and two other antibodies for Cx30. In general, all these antibodies provided immunostaining of granules (dubbed herein puncta), most of them of approximately 0.5 to 2  $\mu\text{m}$  in diameter, with negligible background staining (Figures 1(a) and (b) and 2(a) and (b)). We chose a monoclonal antibody for Cx43 and a polyclonal antibody to Cx30 for immunodetection of the corresponding connexins. In previous studies, we found that, as compared to sections from paraformaldehyde-perfused and post-fixed brains, immunolabeling of Cx43 and Cx30 aggregates is best when performed on brain sections cut fresh-frozen and fixed briefly (15 min) only after they are mounted on slides and immediately preceding the procedure for immunohistochemical detection. Under these conditions, we found that the packing density of both Cx43 (Figure 1) and Cx30 (Figure 2) puncta were dramatically lower in the CUS-exposed group as compared to the control, CUS-naïve group (Cx43 in PLC by 22% and in OFC by 36%; Cx30 in PLC by 38% and in OFC by 40%), with no overlap of values between CUS and control groups (Figures 1 and 2).

### *MBP Area Fraction*

To determine the area fraction of MBP immunoreactivity, we first compared the ability of three different primary antibodies (raised in rabbit, mouse, and chicken) to label myelinated fibers with the minimum background or labeling of structures known not to contain MBP. The best results were obtained with antibodies raised in chicken to MBP (see "Methods" section), and consequently, these were used to determine the area fraction of MBP immunoreactivity in the gray matter of the PLC and OFC. Measurements of MBP area fraction did not include the white matter because the intensity of immunoreactivity in white matter was maximal and appeared

saturated in all animals making it difficult to reliably detect putative differences in MBP-labeling based myelination between experimental subjects. That is, due to the relatively sparser MBP immunostaining in gray matter, it was possible to determine whether there are differences in the extent of myelinated fibers as reflected in the area fraction of immunoreactivity. As illustrated in Figures 3 and 4, the mean area fraction of immunoreactivity was significantly lower in the CUS-exposed group of rats as compared to the control, CUS-naïve group by 24% in the PLC (Figure 3) and 17% in the OFC (Figure 4).

### *Correlation of MBP Immunoreactivity With Cx43 and Cx30 Puncta Packing Density*

Correlation analysis of MBP area fraction versus Cx43 or Cx30 puncta density using all animals in the study showed a significant correlation between MBP area fraction and Cx43 puncta density in the OFC (Figure 5(b)) and between MBP area fraction and Cx30 puncta density in the PLC (Figure 5(c)). It was not possible to determine such a correlation in control subjects alone because the variances of MBP area fraction and Cx43 puncta density were very small and the number of subjects insufficient.

**Behavioral Tests.** In the six animals with CUS used in this research, CUS significantly increased the mean latency to feed in a novel environment, as compared to the six control rats ( $t = 7.356$ ,  $df = 10$ ,  $p < 0.0001$ ). However, CUS did not significantly alter sucrose preference (measured as the ratio of 3% sucrose to plain water) in comparison to control rats ( $t = 1.726$ ,  $df = 10$ ,  $p = 0.1151$ ). The body weight after four weeks of CUS was 7% lower in CUS group ( $407.5 \pm 10.63$ ) as compared to the control group ( $435.6 \pm 9.297$ ), but this difference was not significant ( $t = 1.995$ ,  $df = 10$ ,  $p = 0.07$ ).

**Correlation of Behavioral Parameters With Cx43, Cx30, and MBP Immunoreactivity.** Correlation analysis of behavioral parameters (novelty suppressed feeding latency and ratio of sucrose/water) versus Cx43 or Cx30 puncta density or MBP area fraction using all animals in the study showed significant negative correlation between novelty suppressed feeding latency and Cx43 puncta density in the PLC ( $r = -0.7836$ ,  $p = 0.0043$ ) and OFC ( $r = -0.8369$ ,  $p = 0.0025$ ) (Figure 6(a) and (b)). Similar significant correlations were also found between novelty suppressed feeding latency and Cx30 puncta density in the PLC ( $r = -0.8406$ ,  $p = 0.0006$ ) and OFC ( $r = -0.6428$ ,  $p = 0.0242$ ) (Figure 6(c) and (d)) as well as MBP area fraction in the OFC ( $r = -0.7522$ ,  $p = 0.0076$ ) (Figure 7(a)). It was not possible to determine such a correlation in CUS subjects alone for latency to novelty suppressed feeding because the latency to feeding in all CUS subjects was the same, that is, maximal within the



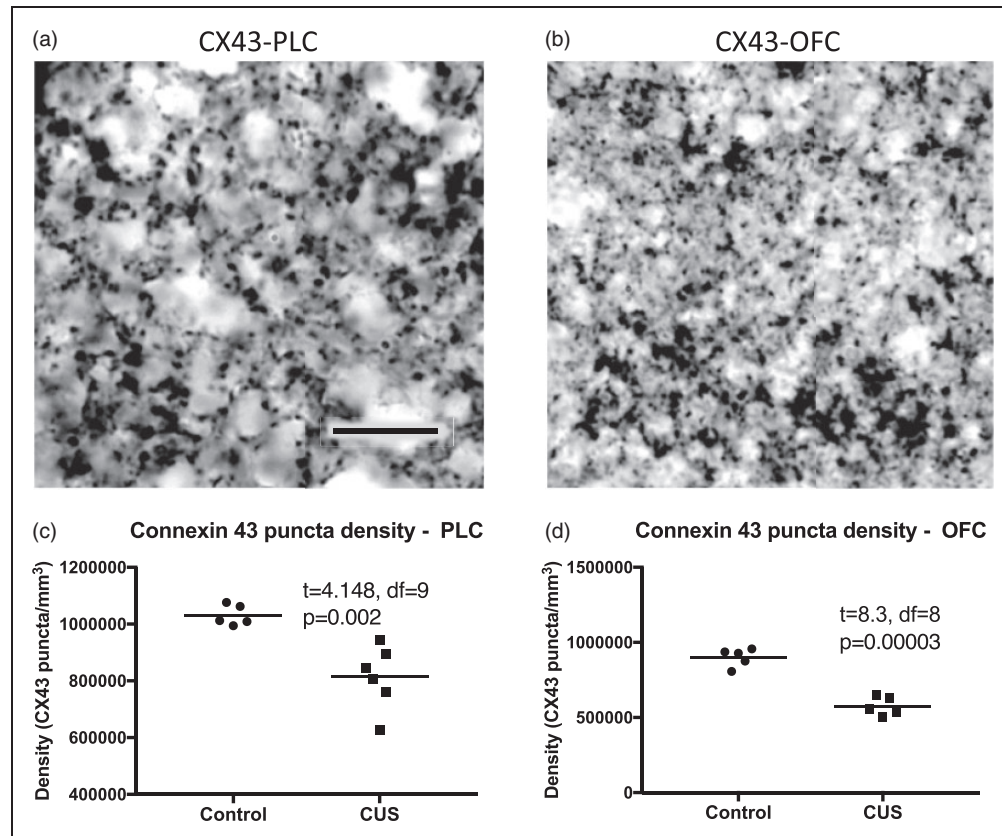


**Figure 1.** Micrographs of CX43 immunoreactive puncta (dark granules in panels (a) for PLC and (b) for OFC) and graphs of CX43 puncta densities in the PLC (c) and OFC (d) of control and CUS-treated rats. The calibration bar in (a) (10 μm) applies to both (a) and (b).

period allowed to interacting with food. In addition, a significant negative correlation was found between the ratio of sucrose/water and Cx30 puncta density in the PLC ( $-0.5787$ ,  $p=0.0487$ ) when all animals were combined (Figure 7(b)). This correlation was also significant in the CUS group alone ( $r=-0.8988$ ,  $p=0.0148$ ) (Figure 7(c)) but not in the control group ( $r=0.2455$ ,  $p=0.6392$ ).

## Discussion

The present results show a dramatic reduction of puncta immunoreactive for astrocyte connexins Cx43 and Cx30, and a reduction as well in the area fraction of immunoreactivity for the myelin marker MBP in the gray matter of two well-differentiated prefrontal areas (PLC and OFC) of rats subjected to CUS, a procedure known to induce depression-like behaviors. In the PLC, a previous study using a two-dimensional counting method found a decrease of Cx43 puncta together with decreases in the levels of Cx43 protein itself and its mRNA in CUS rats as compared to controls.<sup>19</sup> This study further shows that a three-dimensional counting technique using the stereological optical disector rules also allowed the detection of a drastic and consistent decrease of Cx43 immunoreactive puncta in CUS-exposed rats as compared to controls not

only in the PLC, but also in the OFC. In addition, we found that the strong decreases of immunoreactive puncta also affected another major astrocyte connexin, Cx30, in both the PLC and the OFC. The marked decrease of Cx43 and Cx30 puncta in the CUS rat model of depression-like behavior further suggests that prolonged unpredictable stress may play a major role in reducing astrocytic gap junction function because immunoreactive granules or puncta represent actual gap junction aggregates or accumulation of connexons both in gray and white matter<sup>35–37</sup> and some experiments have shown that intercellular spread of dyes small enough to traverse gap junctions is inhibited in the PLC of CUS rats as compared to CUS-naïve rats.<sup>19</sup> Stress-related reductions in connexins may explain the drastic decreases in protein and mRNA levels for Cx43 and Cx30 in dorso-lateral PFC found by Ernst et al.<sup>15</sup> in depressed human subjects dying by suicide and the similarly low immunoreactive puncta density and levels of Cx43 that we have detected in the OFC of MDD subjects.<sup>16</sup> Because a variety of factors can contribute to the development of MDD, it cannot be ruled out that decrease of connexins is further influenced by factors other than stress. For instance, neuronal activity disturbances present in MDD and connexin expression may directly regulate

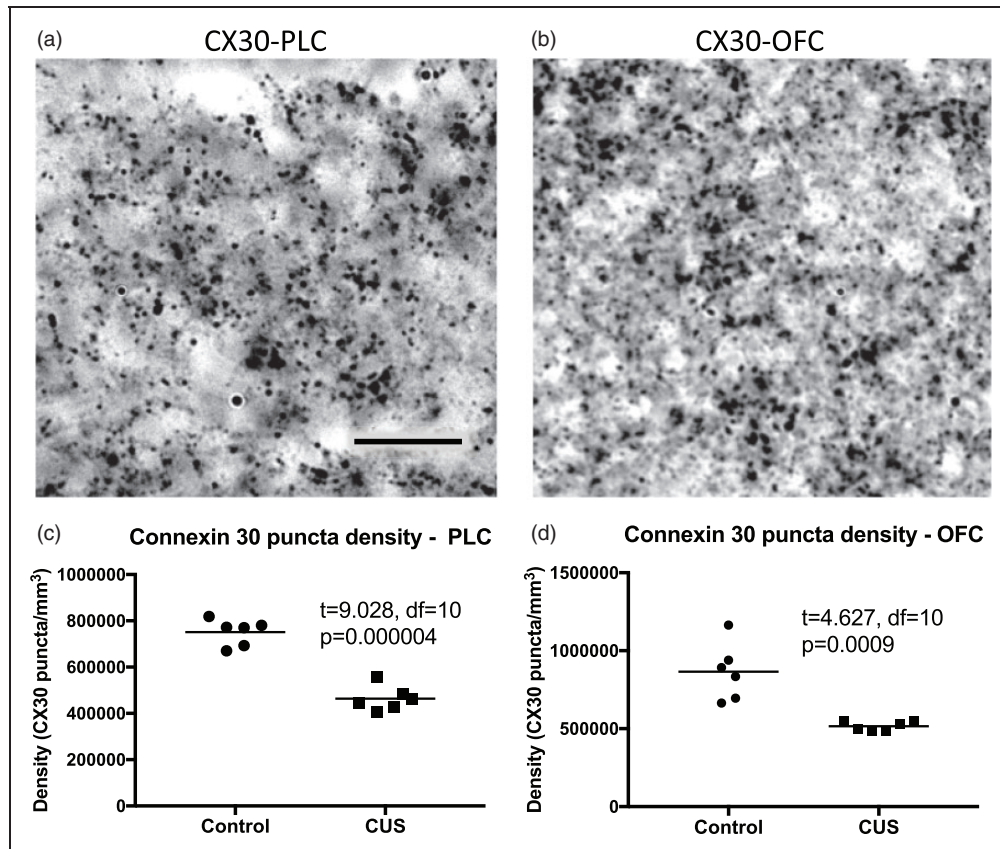


**Figure 2.** Micrographs of CX30 immunoreactive puncta (dark granules in panels (a) for PLC and (b) for OFC) and graphs of CX30 puncta densities in the PLC (c) and OFC (d) of control and CUS-treated rats. The calibration bar in (a) (10 μm) applies to both (a) and (b).

the expression of Cx43.<sup>38</sup> Future studies in animal models should examine which combination of factors may regulate the recently discovered connexin changes in MDD.

The current results suggest that disturbances of gap junction communication may occur not only in the PLC but also in the OFC of stress-exposed rats. These two brain areas are involved in well-differentiated aspects of cognitive, emotional, and behavioral control, making it possible that the disruption of the normal distribution of gap junctions by stress in the two areas contributes to the variety of functional and behavioral domains that are altered in subjects with depression. In addition, low Cx43 and Cx30 after CUS in both rat PLC and OFC suggests that reduced astrocytic gap junction density may generalize to the entire PFC.

The involvement of both Cx43 and Cx30 points to overall gap junction communication as a major glial mechanism in the effects of stress on prefrontal function, but the involvement of noncoupled connexons, also known as hemichannels, cannot be yet dismissed. Cx43 antibodies may also detect Cx43 hemichannel aggregates in astrocyte cell membranes, which do not form gap junctions. Interestingly, relatively short exposure to antidepressants is capable of variably reducing the function

of activated Cx43 hemichannels.<sup>39</sup> After longer exposures, antidepressants seem to increase the expression of Cx43 in vivo and in astrocyte cultures, but both acute and long-term actions on the function of gap junction and hemichannel vary with the type of antidepressant.<sup>39</sup> On the other hand, it must be kept in mind that Cx30 does not appear to form hemichannels in the brain,<sup>40</sup> so Cx30's putative participation in the prefrontal pathophysiology of depression would not depend on hemichannel activity.

Simply detecting changes of Cx43 and Cx30 expression or distributions is clearly insufficient to understand the respective contributions of hemichannels and gap junction aggregates in glia-related functional changes in depression-like behavior. Communication among astrocytes and of these with other cell types depends not only on gap junctions but also on the hemichannels' role in the release of gliotransmitters to the extracellular space.<sup>41–44</sup> Further research will be needed to determine whether hemichannels' disturbance is involved in the effects of reduced connexins in the PFC and which is their contribution as compared to Cx43 and Cx30-containing gap junctions.

Reductions in astrocyte connexins are accompanied by a decrease in the area fraction of MBP immunoreactivity



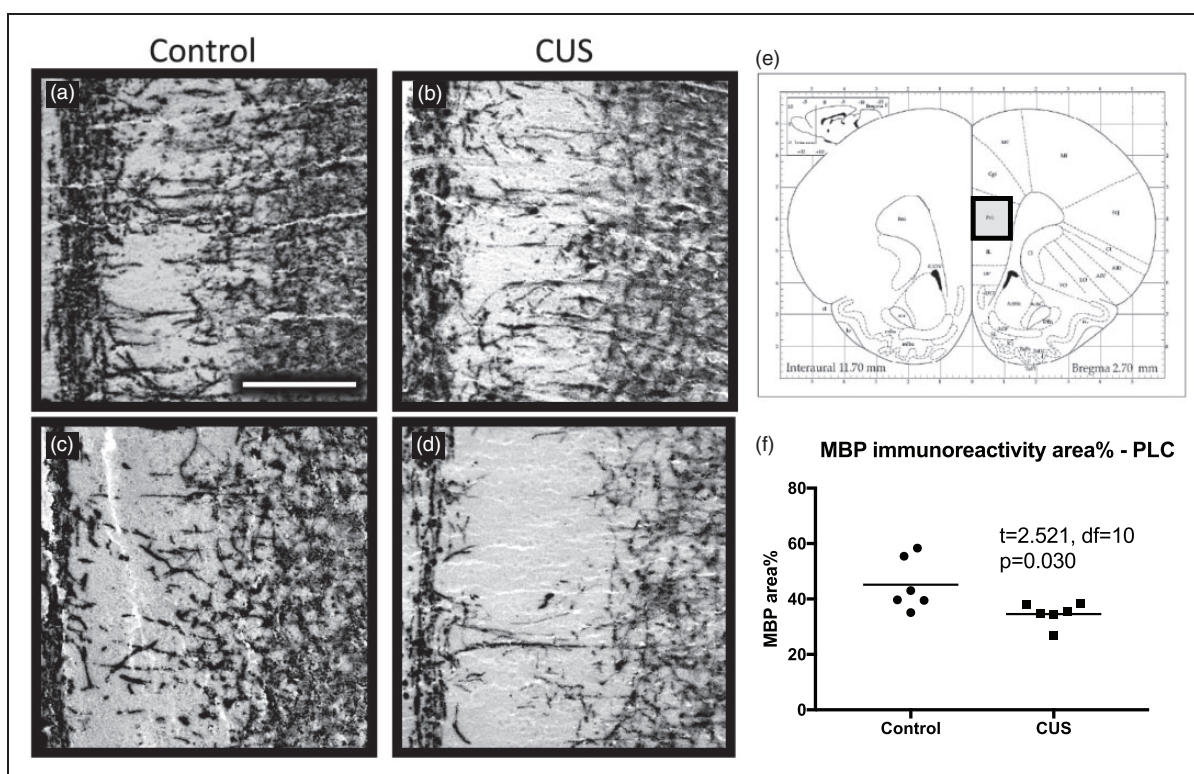


**Figure 3.** Micrographs of MBP immunoreactivity (darkly stained structures) in the PLC of 2 control (a and b) and 2 CUS-treated rats (c and d) and graph of the MBP area fraction values in the same groups of rats (f). Panel (e) shows a representative PLC location where micrographs were taken in coronal sections of the rat brain. The calibration bar in (a) (500  $\mu$ m) applies to (a) to (d).

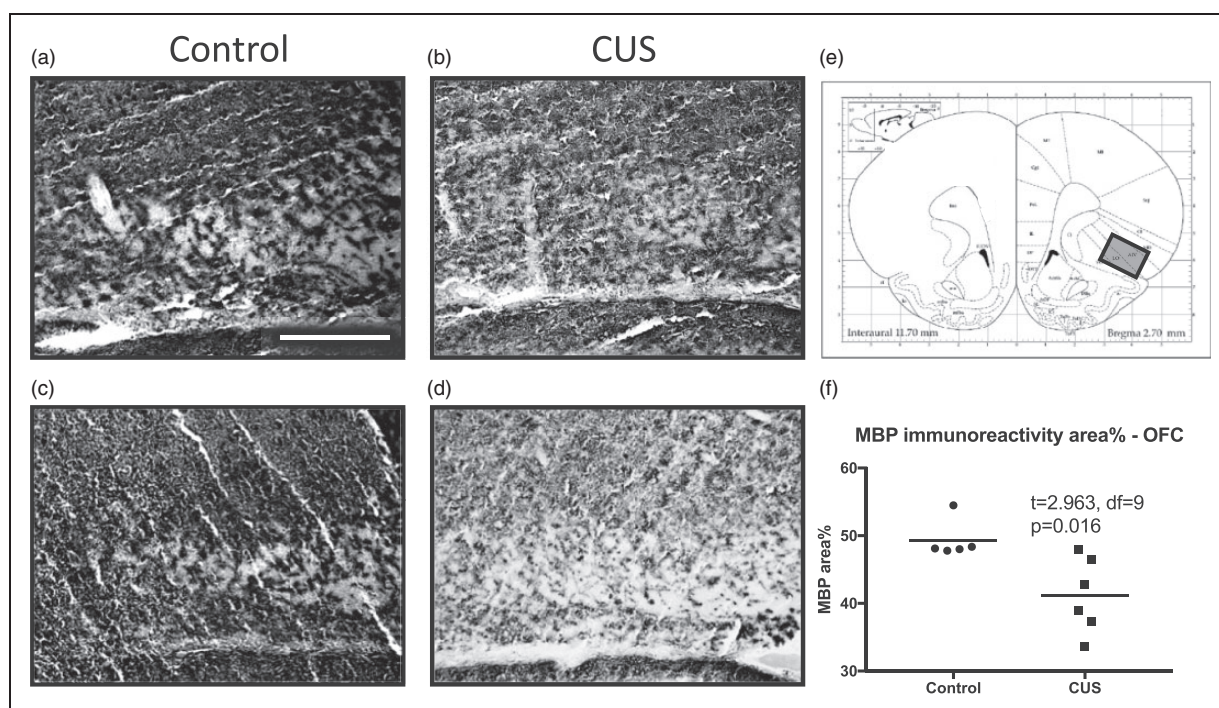


**Figure 4.** Micrographs of MBP immunoreactivity (darkly stained structures) in the OFC of 2 control (a and b) and 2 CUS-treated rats (c and d), and graph of the MBP area fraction values in the same groups of rats (f). Panel (e) shows a representative OFC location where micrographs were taken in coronal sections of the rat brain. The calibration bar in (a) (500  $\mu$ m) applies to (a) to (d).

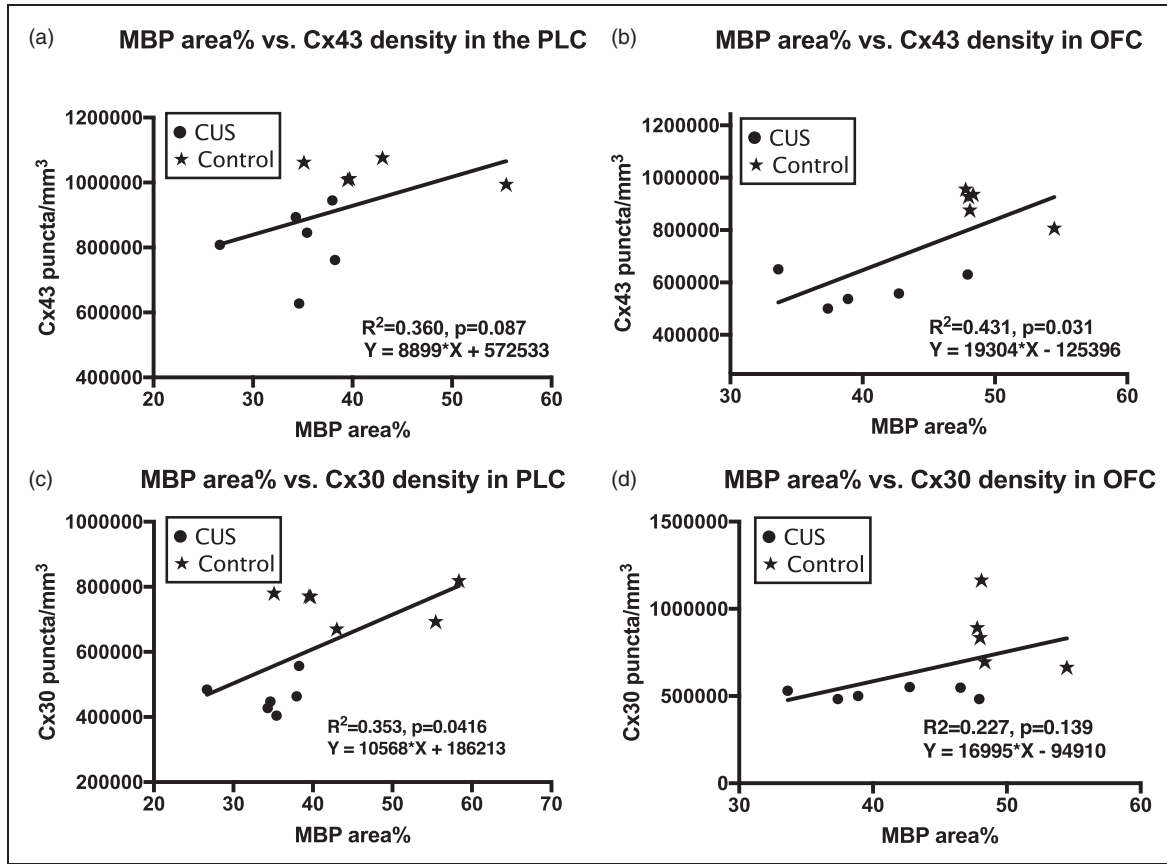


**Figure 5.** Graphs illustrating the correlation analysis between MBP area fraction and the packing density of CX43 puncta in PLC (a) and OFC (b) or CX30 puncta in PLC (c) and OFC (d) of the rat brain.

in the PLC and OFC of rats subjected to CUS suggesting that prolonged stress causes alteration in myelination parameters including the extent of MBP immunostaining in the gray matter. A similar decrease in myelin markers has been detected in the PLC of mice subjected to chronic social defeat, another model of prolonged stress,<sup>30</sup> suggesting that the effects of repeated stress on behavior and emotional regulation may be mediated at least partly by reductions in myelin maintenance in the PLC and, according to the present data, in the OFC. Using electron microscopic (EM) measurements of myelin thickness other researchers have shown that social isolation of mice for four weeks causes a thinning of myelin sheaths in the white matter at prefrontal levels but not in more posterior levels of the corpus callosum or in the hippocampus.<sup>20</sup> Likewise, one EM study of the infralimbic portion of the PFC in rats subjected to chronic mild stress has demonstrated a decrease in the density of myelinated axonal profiles as compared to control, nonstressed rats.<sup>45</sup> Clearly, both neurochemical and EM ultrastructural approaches, although pointing in the same direction (disrupted myelination markers), used different indices of myelin integrity and different models of stress. Thus, it will be necessary to determine if CUS also results in

reduced thickness of the myelin sheath or if reduced MBP labeling is reversible after allowing enough time for recovery after CUS.

The fact that two different prefrontal areas show a decrease of MBP area fraction is consistent with depression-like functional disturbances described in both areas after CUS in rodents<sup>29,46–48</sup> and also with pathological and physiological findings in the approximately homologous cortical regions in MDD.<sup>49–51</sup> In MDD, there are also gene expression and protein studies showing decreases of mRNA or protein levels of myelin component or transcription factors related to the expression of those proteins.<sup>17,18,52</sup> Thus, structural and neurochemical alterations in extant myelin and the oligodendrocytes that form it may explain the reduction in MBP area fraction in this study.

Repeated stress or prolonged high corticosterone levels in rodents may also cause a decrease in the number and morphological abnormalities in NG2 cells in the PFC<sup>53–57</sup> while low numbers of these cells are present in the PFC of human subjects with MDD.<sup>57</sup> NG2 cells act as oligodendrocyte precursors and can be activated to differentiate into oligodendrocytes. Thus, decreases in NG2 cells may also contribute to a net reduction of



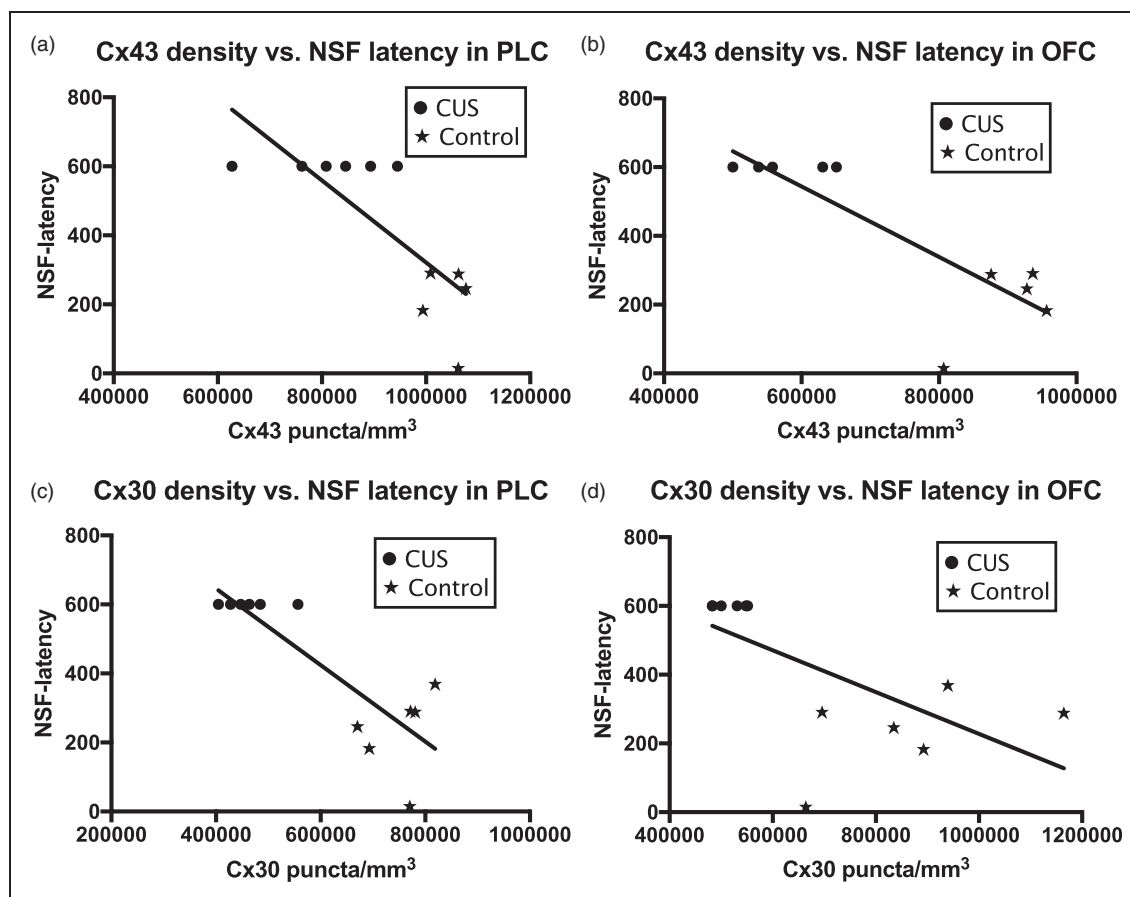


**Figure 6.** Scatter plots with regression lines illustrating the correlation of connexin 43 (a and b) and connexin 30 (c and d) puncta density in PLC and OFC with the latency to feed in a novel environment for all of the subjects combined. Controls and CUS-treated rats are distinguished by stars and round dots, respectively. NSF: novelty suppressed feeding.

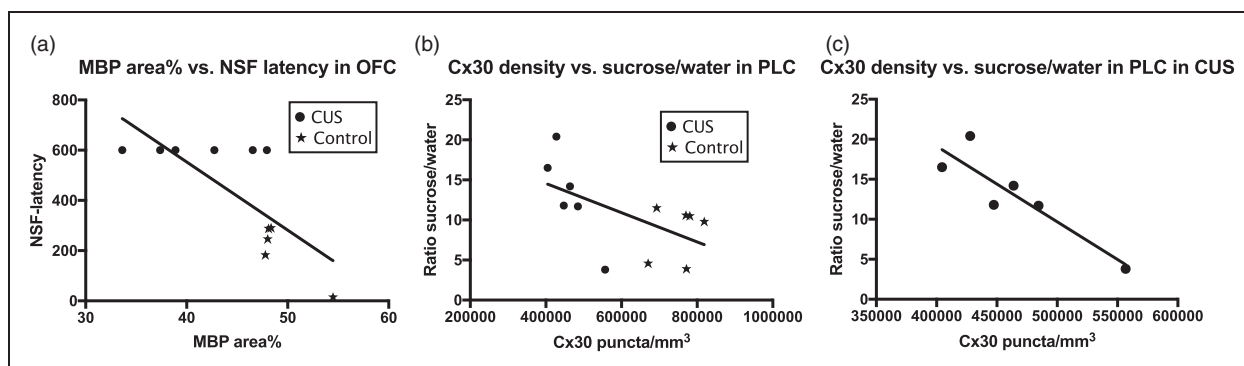


**Figure 7.** Scatter plots with regression lines illustrating: (a) the correlation of MBP area fraction of immunoreactivity with latency to feed, (b) the correlation of connexin 30 and the ratio of consumption of an aqueous 3% sucrose solution versus plain water for all the subjects of the study combined, and (c) the same correlation only for CUS-treated rats. Controls and CUS-treated rats are distinguished as in Figure 6. MBP: myelin basic protein; NSF: novelty suppressed feeding.

MBP positive fibers if there are less NG2 cells differentiating into myelinating oligodendrocytes. At the moment it cannot be ruled out that impaired maintenance of extant myelin and diminished replacement of

myelinating oligodendrocytes by NG2 cells sum up to cause the reduction in MBP area fraction observed in this study, and future studies should ascertain if this is the case.

Concurrent reduction of Cx43-, Cx30-, and MBP-immunolabeled structures is consistent with a mechanism linking changes in astrocyte gap junction proteins and disturbed myelin morphology in depression. Part of the concurrent effects could be related to repeated elevations of corticosterone that are associated with the stress response because corticosteroids or their metabolites may act on glucocorticoid or mineralocorticoid receptors in astrocytes and oligodendrocytes and reduce specific astrocyte and myelin markers.<sup>58–60</sup> In cultured astrocytes activation of these receptors can induce a reduction in the expression of connexins,<sup>59,61,62</sup> while activation of the same receptors in oligodendrocytes or their precursors can result in deficient myelination or MBP expression,<sup>58</sup> although the effects of corticosteroids on oligodendrocytes and myelination may be dependent on the developmental stage or the brain region.<sup>63,64</sup> It is also possible that the *in vivo* effect of stress on the expression of myelin markers is mediated by the reduction of Cx43 and/or Cx30 because downregulation of astrocyte connexins results in serious disturbance of myelination in animal models.<sup>22,26</sup> Further research is necessary to determine whether and how connexin-independent and connexin-mediated effects of stress on myelination play a role in depression and stress-related disorders.

## Conclusion

Low Cx43 and Cx30 after CUS in rat PLC and OFC suggests that reduced astrocytic gap junction density may generalize to the entire PFC. Concurrent reduction of Cx43-, Cx30-, and MBP-immunolabeled structures is consistent with a mechanism linking changes in astrocyte gap junction proteins and disturbed myelin morphology in depression.

## Declaration of Conflicting Interests

The author(s) declared no potential conflicts of interest with respect to the research, authorship, and/or publication of this article.

## Funding

The author(s) disclosed receipt of the following financial support for the research, authorship, and/or publication of this article: NIMH grant R56MH113828, Animal Behavior and Imaging Cores of NIGMS grant P30GM103328, and IRSP grants from the University of Mississippi Medical Center.

## ORCID iD

José Javier Miguel-Hidalgo  <http://orcid.org/0000-0002-4094-1249>

## References

1. Kendler KS, Gardner CO, Prescott CA. Clinical characteristics of major depression that predict risk of depression in relatives. *Arch Gen Psychiatry* 1999; 56: 322–327.
2. Mahar I, Bambico FR, Mechawar N, et al. Stress, serotonin, and hippocampal neurogenesis in relation to depression and antidepressant effects. *Neurosci Biobehav Rev* 2014; 38: 173–192.
3. Swaab DF, Bao AM, Lucassen PJ. The stress system in the human brain in depression and neurodegeneration. *Ageing Res Rev*. 2005; 4: 141–194.
4. Hammen C. Stress and depression. *Ann Rev Clin Psychol*. 2005; 1: 293–319.
5. Willner P. Validity, reliability and utility of the chronic mild stress model of depression: a 10-year review and evaluation. *Psychopharmacology (Berl)* 1997; 134: 319–329.
6. Katz RJ, Sibel M. Animal model of depression: tests of three structurally and pharmacologically novel antidepressant compounds. *Pharmacol Biochem Behav*. 1982; 16: 973–977.
7. Mineur YS, Belzung C, Crusio WE. Effects of unpredictable chronic mild stress on anxiety and depression-like behavior in mice. *Behav Brain Res* 2006; 175: 43–50.
8. Elizalde N, Garcia-Garcia AL, Totterdell S, et al. Sustained stress-induced changes in mice as a model for chronic depression. *Psychopharmacology (Berl)*. 2010; 210: 393–406.
9. Banasr M, Chowdhury GM, Terwilliger R, et al. Glial pathology in an animal model of depression: reversal of stress-induced cellular, metabolic and behavioral deficits by the glutamate-modulating drug riluzole. *Mol Psychiatry*. 2010; 15: 501–511.
10. Rajkowska G, Miguel-Hidalgo JJ, Wei JR, et al. Morphometric evidence for neuronal and glial prefrontal cell pathology in major depression. *Biol Psychiatry*. 1999; 45: 1085–1098.
11. Rajkowska G, Miguel-Hidalgo JJ. Gliogenesis and glial pathology in depression. *CNS Neurol Disord Drug Targets*. 2007; 6: 219–233.
12. Miguel-Hidalgo JJ, Waltzer R, Whittom AA, et al. Glial and glutamatergic markers in depression, alcoholism, and their comorbidity. *J Affect Disord*. 2010; 127: 230–240.
13. Cotter DR, Pariante CM, Everall IP. Glial cell abnormalities in major psychiatric disorders: the evidence and implications. *Brain Res Bull*. 2001; 55: 585–595.
14. Banasr M, Duman RS. Glial loss in the prefrontal cortex is sufficient to induce depressive-like behaviors. *Biol Psychiatry*. 2008; 64: 863–870.
15. Ernst C, Nagy C, Kim S, et al. Dysfunction of astrocyte connexins 30 and 43 in dorsal lateral prefrontal cortex of suicide completers. *Biol Psychiatry*. 2011; 70: 312–319.
16. Miguel-Hidalgo JJ, Wilson BA, Hussain S, et al. Reduced connexin 43 immunolabeling in the orbitofrontal cortex in alcohol dependence and depression. *J Psychiatr Res*. 2014; 55: 101–109.
17. Rajkowska G, Mahajan G, Maciag D, et al. Oligodendrocyte morphometry and expression of myelin-related mRNA in ventral prefrontal white matter in major depressive disorder. *J Psychiatr Res*. 2015; 65: 53–62.
18. Miguel-Hidalgo JJ, Hall KO, Bonner H, et al. MicroRNA-21: expression in oligodendrocytes and correlation with low myelin mRNAs in depression and alcoholism. *Prog Neuropsychopharmacol Biol Psychiatry*. 2017; 79: 503–514.

19. Sun JD, Liu Y, Yuan YH, et al. Gap junction dysfunction in the prefrontal cortex induces depressive-like behaviors in rats. *Neuropsychopharmacology*. 2012; 37: 1305–1320.
20. Liu J, Dietz K, Deloyht JM, et al. Impaired adult myelination in the prefrontal cortex of socially isolated mice. *Nat Neurosci*. 2012; 15: 1621–1623.
21. Miyata S, Taniguchi M, Koyama Y, et al. Association between chronic stress-induced structural abnormalities in Ranvier nodes and reduced oligodendrocyte activity in major depression. *Sci Rep*. 2016; 6: 23084.
22. Nualart-Marti A, Solsona C, Fields RD. Gap junction communication in myelinating glia. *Biochim Biophys Acta*. 2013; 1828: 69–78.
23. Edgar N, Sibille E. A putative functional role for oligodendrocytes in mood regulation. *Transl Psychiatry*. 2012; 2: e109.
24. Gao Y, Ma J, Tang J, et al. White matter atrophy and myelinated fiber disruption in a rat model of depression. *J Comp Neurol* 2017; 525: 1922–1933.
25. Orthmann-Murphy JL, Abrams CK, Scherer SS. Gap junctions couple astrocytes and oligodendrocytes. *J Mol Neurosci* 2008; 35: 101–116.
26. Lutz SE, Zhao Y, Gulinello M, et al. Deletion of astrocyte connexins 43 and 30 leads to a dysmyelinating phenotype and hippocampal CA1 vacuolation. *J Neurosci* 2009; 29: 7743–7752.
27. Nave KA. Myelination and the trophic support of long axons. *Nat Rev Neurosci* 2010; 11: 275–283.
28. Fields RD. A new mechanism of nervous system plasticity: activity-dependent myelination. *Nat Rev Neurosci* 2015; 16: 756–767.
29. Holmes A, Wellman CL. Stress-induced prefrontal reorganization and executive dysfunction in rodents. *Neurosci Biobehav Rev* 2009; 33: 773–783.
30. Lehmann ML, Weigel TK, Elkahloun AG, et al. Chronic social defeat reduces myelination in the mouse medial prefrontal cortex. *Sci Rep* 2017; 7: 46548.
31. Zheng C, Quan M, Zhang T. Decreased thalamo-cortical connectivity by alteration of neural information flow in theta oscillation in depression-model rats. *J Comput Neurosci* 2012; 33: 547–558.
32. Qiao H, Li MX, Xu C, et al. Dendritic spines in depression: what we learned from animal models. *Neural Plast* 2016; 2016: 8056370.
33. Rajkowska G, Legutko B, Moulana M, et al. Astrocyte pathology in the ventral prefrontal white matter in depression. *J Psychiatr Res* 2018; 102: 150–158.
34. Riaz MS, Bohlen MO, Gunter BW, et al. Attenuation of social interaction-associated ultrasonic vocalizations and spatial working memory performance in rats exposed to chronic unpredictable stress. *Physiol Behav* 2015; 152: 128–134.
35. Nagy JI, Yamamoto T, Sawchuk MA, et al. Quantitative immunohistochemical and biochemical correlates of connexin43 localization in rat brain. *Glia* 1992; 5: 1–9.
36. Yamamoto T, Ochalski A, Hertzberg EL, et al. On the organization of astrocytic gap junctions in rat brain as suggested by LM and EM immunohistochemistry of connexin43 expression. *J Comp Neurol* 1990; 302: 853–883.
37. Segretain D, Falk MM. Regulation of connexin biosynthesis, assembly, gap junction formation, and removal. *Biochimica et Biophysica Acta (BBA) – Biomembranes* 2004; 1662: 3–21.
38. Rouach N, Glowinski J, Giaume C. Activity-dependent neuronal control of gap-junctional communication in astrocytes. *J Cell Biol* 2000; 149: 1513–1526.
39. Jeanson T, Pondaven A, Ezan P, et al. Antidepressants Impact Connexin 43 channel functions in astrocytes. *Front Cell Neurosci* 2015; 9: 495.
40. Giaume C, Leybaert L, Naus CC, et al. Connexin and pannexin hemichannels in brain glial cells: properties, pharmacology, and roles. *Front Pharmacol* 2013; 4: 88.
41. Ye ZC, Wyeth MS, Baltan-Tekkok S, et al. Functional hemichannels in astrocytes: a novel mechanism of glutamate release. *J Neurosci* 2003; 23: 3588–3596.
42. Abudara V, Roux L, Dallerac G, et al. Activated microglia impairs neuroglial interaction by opening Cx43 hemichannels in hippocampal astrocytes. *Glia* 2015; 63: 795–811.
43. Kang J, Kang N, Lovatt D, et al. Connexin 43 hemichannels are permeable to ATP. *J Neurosci* 2008; 28: 4702–4711.
44. Orellana JA, Moraga-Amaro R, Diaz-Galarce R, et al. Restraint stress increases hemichannel activity in hippocampal glial cells and neurons. *Front Cell Neurosci* 2015; 9: 102.
45. Csabai D, Wiborg O, Czeh B. Reduced synapse and axon numbers in the prefrontal cortex of rats subjected to a chronic stress model for depression. *Front Cell Neurosci* 2018; 12: 24.
46. McKlveen JM, Morano RL, Fitzgerald M, et al. Chronic stress increases prefrontal inhibition: a mechanism for stress-induced prefrontal dysfunction. *Biol Psychiatry* 2016; 80: 754–764.
47. Yuen EY, Wei J, Liu W, et al. Repeated stress causes cognitive impairment by suppressing glutamate receptor expression and function in prefrontal cortex. *Neuron* 2012; 73: 962–977.
48. McEwen BS, Morrison JH. The brain on stress: vulnerability and plasticity of the prefrontal cortex over the life course. *Neuron* 2013; 79: 16–29.
49. Feyissa AM, Chandran A, Stockmeier CA, et al. Reduced levels of NR2A and NR2B subunits of NMDA receptor and PSD-95 in the prefrontal cortex in major depression. *Prog Neuropsychopharmacol Biol Psychiatry* 2009; 33: 70–75.
50. Feyissa AM, Woolverton WL, Miguel-Hidalgo JJ, et al. Elevated level of metabotropic glutamate receptor 2/3 in the prefrontal cortex in major depression. *Prog Neuropsychopharmacol Biol Psychiatry* 2010; 34: 279–283.
51. Jernigan CS, Goswami DB, Austin MC, et al. The mTOR signaling pathway in the prefrontal cortex is compromised in major depressive disorder. *Prog Neuropsychopharmacol Biol Psychiatry* 2011; 35: 1774–1779.
52. Regenold WT, Phatak P, Marano CM, et al. Myelin staining of deep white matter in the dorsolateral prefrontal cortex in schizophrenia, bipolar disorder, and unipolar major depression. *Psychiatry Res* 2007; 151: 179–188.
53. Banasr M, Valentine GW, Li XY, et al. Chronic unpredictable stress decreases cell proliferation in the cerebral cortex of the adult rat. *Biol Psychiatry* 2007; 62: 496–504.



54. Czeh B, Muller-Keuker JI, Rygula R, et al. Chronic social stress inhibits cell proliferation in the adult medial prefrontal cortex: hemispheric asymmetry and reversal by fluoxetine treatment. *Neuropsychopharmacology* 2007; 32: 1490–1503.
55. Alonso G. Prolonged corticosterone treatment of adult rats inhibits the proliferation of oligodendrocyte progenitors present throughout white and gray matter regions of the brain. *Glia* 2000; 31: 219–231.
56. Yang Y, Zhang Y, Luo F, et al. Chronic stress regulates NG2(+) cell maturation and myelination in the prefrontal cortex through induction of death receptor 6. *Exp Neurol* 2016; 277: 202–214.
57. Birey F, Kloc M, Chavali M, et al. Genetic and stress-induced loss of NG2 glia triggers emergence of depressive-like behaviors through reduced secretion of FGF2. *Neuron* 2015; 88: 941–956.
58. Melcangi RC, Magnaghi V, Cavarretta I, et al. Corticosteroid effects on gene expression of myelin basic protein in oligodendrocytes and of glial fibrillary acidic protein in type 1 astrocytes. *J Neuroendocrinol* 1997; 9: 729–733.
59. Xia CY, Wang ZZ, Zhang Z, et al. Corticosterone impairs gap junctions in the prefrontal cortical and hippocampal astrocytes via different mechanisms. *Neuropharmacology* 2018; 131: 20–30.
60. Crossin KL, Tai MH, Krushel LA, et al. Glucocorticoid receptor pathways are involved in the inhibition of astrocyte proliferation. *Proc Natl Acad Sci U S A* 1997; 94: 2687–2692.
61. Xia CY, Chu SF, Zhang S, et al. Ginsenoside Rg1 alleviates corticosterone-induced dysfunction of gap junctions in astrocytes. *J Ethnopharmacol* 2017; 208: 207–213.
62. Carter BS, Hamilton DE, Thompson RC. Acute and chronic glucocorticoid treatments regulate astrocyte-enriched mRNAs in multiple brain regions in vivo. *Front Neurosci* 2013; 7: 139.
63. Chetty S, Friedman AR, Taravosh-Lahn K, et al. Stress and glucocorticoids promote oligodendrogenesis in the adult hippocampus. *Mol Psychiatry* 2014; 19: 1275–1283.
64. Mann SA, Versmold B, Marx R, et al. Corticosteroids reverse cytokine-induced block of survival and differentiation of oligodendrocyte progenitor cells from rats. *J Neuroinflammation* 2008; 5: 39.